BRNO UNIVERSITY OF TECHNOLOGY

VYSOKÉ UČENÍ TECHNICKÉ V BRNĚ

FACULTY OF MECHANICAL ENGINEERING

FAKULTA STROJNÍHO INŽENÝRSTVÍ

INSTITUTE OF SOLID MECHANICS, MECHATRONICS AND BIOMECHANICS

ÚSTAV MECHANIKY TĚLES, MECHATRONIKY A BIOMECHANIKY

CONSTITUTIVE MODELLING OF COMPOSITES WITH ELASTOMER MATRIX AND FIBRES WITH SIGNIFICANT BENDING STIFFNESS

KONSTITUTIVNÍ MODELOVÁNÍ KOMPOZITŮ S ELASTOMEROVOU MATRICÍ A VLÁKNY S VÝZNAMNOU OHYBOVOU TUHOSTÍ

DOCTORAL THESIS SHORT VERSION

TEZE DIZERTAČNÍ PRÁCE

AUTHOR — Ing. Svitlana Fedorova

AUTOR PRÁCE

SUPERVISOR — prof. Ing. Jiří Burša, Ph.D.

ŠKOLITEL

CO-SUPERVISOR — Ing. Pavel Skácel, PhD

ŠKOLITEL SPECIALISTA

BRNO 2018

Abstract

Constitutive modelling of fibre reinforced solids is the focus of this work. To account for the resulting anisotropy of material, the corresponding strain energy function contains additional terms. Thus, tensile stiffness in the fibre direction is characterised by additional strain invariant and respective material constant. In this way deformation in the fibre direction is penalised.

Following this logic, the model investigated in this work includes the term that penalises change in curvature in the fibre direction. The model is based on the large strain anisotropic formulation involving couple stresses, also referred to as "polar elasticity for fibre reinforced solids". Mechanical tests are carried out to confirm the limits of applicability of the classical elasticity for constitutive description of composites with thick fibres.

The specific simplified model is chosen, which involves new kinematic quantities related to fibre curvature and the corresponding material stiffness parameters. In particular, additional constant k_3 (associated with the fibre bending stiffness) is considered. Within the small strains framework, k_3 is analytically linked to the geometric and material properties of the composite and can serve as a parameter augmenting the integral stiffness of the whole plate. The numerical tests using the updated finite element code for couple stress theory confirm the relevance of this approach. An analytical study is also carried out, extending the existing solution by Farhat and Soldatos for the fibre-reinforced plate, by including additional extra moduli into constitutive description.

Solution for a pure bending problem is extended analytically for couple stress theory. Size effect of fibres is observed analytically.

Verification of the new constitutive model and the updated code is carried out using new exact solution for the anisotropic couple stress continuum with the incompressibility constraint. Perfect agreement is achieved for small strain case. Large strain problem is considered by finite element method only qualitatively.

Three cases of kinematic constraints on transversely isotropic material are considered in the last section: incompressibility, inextensibility and the double constraint case. They are compared with a general material formulation in which the independent elastic constants are manipulated in order to converge the solution to the "constraint" formulation solution. The problem of a thick plate under sinusoidal load is used as a test problem. The inclusion of couple stresses and additional bending stiffness constant is considered as well. The scheme of determination of the additional constant d_{31} is suggested by using mechanical tests combined with the analytical procedure.

Contents

1. INTRODUCTION

Fibre reinforced composite materials are widely used in automotive and aerospace industries. In particular, fibre-reinforced rubber is being used in pneumatic tyres, air springs, tubings and belt structures. Effective properties of a composite are generally influenced by the properties of constituents, volume fraction and directions of fibres, and quality of adhesion between rubber and fibres. Strength and stiffness in a preferred direction of the composite relate to properties of fibres, while properties of matrix determine material strength under shear, compression, tension perpendicularly to the fibres, and resistance of the composite to fatigue.

In the present work, fibres in the composite are regarded as slender beams embedded in the nonlinear or linear elastic matrix. Employing the kinematics and general constitutive formulation presented in [2] and some newer findings [3], [4], [5], [6], [7], [8], [9] the author investigates a homogeneous model taking both tensile and bending stiffness contributed by fibres into account. The effect of individual fibres is "smeared – out" so that the bending stiffness of the homogeneous model simulates bending behaviour of the real heterogeneous structure.

1.1. Goals of the thesis

The broad objective of the thesis is to extend the existing research concerning constitutive modelling of the fibre-reinforced materials with elastomer matrix with the use of couple stress theory. In this objective the following issues are included:

- realization of mechanical tests to illustrate the limits of applicability of the classical large strain elasticity for constitutive description of composites with thick fibres;
- choice of the strain energy density model on the basis of polar elasticity theory;
- new analytical solutions for polar elasticity or the extension of existing ones;
- modification of FEM formulation;
- verification of FE solutions for some analytically solvable problems;
- theoretical study of the additional elastic constants and their influence.

In the following chapter the works done on these issues are specified in greater detail.

2. STATE OF THE ART

In general, the fibre composite described above can be modelled in two ways. The first way implies explicit geometrical modelling of (linear elastic) fibres embedded in the (hyperelastic or elastic) matrix. Such models will be referred to as “bimaterial models” in this proposal. Alternatively, a so called “unimaterial” model can be employed − it is based on geometry of the whole composite body only (without distinguishing its structural details) and includes phenomenological anisotropic constitutive model. The effect of tensile stiffness contributed by fibres is included mathematically into constitutive equations. Such model is computationally advantageous, but its application is limited.

The use of phenomenological anisotropic models started with Spencer [10]. Anisotropic hyperelastic models typically include strain-energy density as a function of strain invariants with some of the invariants depending on the unit vector (vectors) of the reference fibre direction [11] [12], [13], [14]. In this way an intrinsic assumption of infinitesimally thin, densely and uniformly distributed fibres is implied, leading to their zero bending stiffness. The closer the composite structure is to these assumptions, the better agreement can be provided by the model. Such unimaterial finite strain models have been successfully employed for modelling of rubber reinforced by thin textile or carbon fibres [15], [16], [17], [18], [19], [5], [20]. In general, these models are not applicable if the characteristic length scale of non-homogeneity is comparable with dimensions of the specimen [21] and so called size effects arise. It is often the case when microscale problems [22], [23], [24],[25], [26], [27], [28] or composite materials [21], [29], [30], [31] are considered. The applied classical Cauchy continuum theory is not able to account for the influence of the characteristic size of substructure on material behaviour.

In order to deal with the presence of size effects, non-classical continuum mechanics theories are typically employed. There are two classes of generalized continuum theories: higher-grade and higher-order theories [32]. In brief, higher-grade theories employ higher order gradients of the displacements, while higher-order continuum theories include additional kinematic variables attached to the material point. In particular, Cosserat theory [33], [34] (also known as micropolar) adds independent rotational degrees of freedom to the classical continuum; a detailed review and bibliography of this theory can be found e.g. in Altenbach [35]. Couple stress theory [36], [37] can be regarded as a special case of Cosserat theory, where a connection between the field of rotations and the displacement gradients is present.

In this work the focus is on the fibre reinforced materials with one family of fibres – transversely isotropic material, generally hyperelastic. For such solids with the size effects related to the bending stiffness, a new constitutive framework using CST was developed by Spencer and

Soldatos in 2007 [2]. The authors intended the model to represent the behaviour of the fibre reinforced elastomers when the fibre thickness is comparable with the lowest lateral dimension of the specimen. Constitutive formulation is mathematically based on the notion of deformed fibre curvature, in addition to invariants of the deformation gradient. The introduced theoretical framework allows taking into account the contribution of the individual fibres to the bending stiffness of composite by employing the continuum capable of bearing couple stresses. A subsequent progress in that area was made by Soldatos [37], [38], [39]. This is the framework adopted in the present work.

The latest contribution by Farhat et al [7] should be mentioned as well; it deals with some important analytical solutions within the linear polar elasticity for fibre-reinforced solids.

Adopting the framework of Spencer and Soldatos, Lasota [3] develops a finite element formulation and implementation aimed at solving large strain polar elasticity problems. He also proposes a specific simplified strain energy description.

The aim of the present work is to progress further in understanding and application of the polar elasticity and hyperelasticity for fibre-reinforced solids. The emphasis is on verification and enhancement of both the constitutive model and its FEM implementation.

3. PRELIMINARY STUDY: SPECIMENS WITH NEGLIGIBLE FIBRE BENDING STIFFNESS

3.1. Experimental methods

Uniaxial tension tests of composite specimens with a rubber matrix and single family of textile fibres in the middle layer of the specimen are carried out. Four groups of specimens with different declination of fibres were tested: 0°, 30°, 45°, 90°. All the specimens had dimensions approximately 110×22×2.5 mm and diameter of the fibres 0.8 mm. Tension tests were realized using universal testing machine ZWICK Z020-TND. Elongation in the middle region of the specimen was recorded by extensometers (**Fig. 3.1**); the distance between extensometer levers was 20 mm.

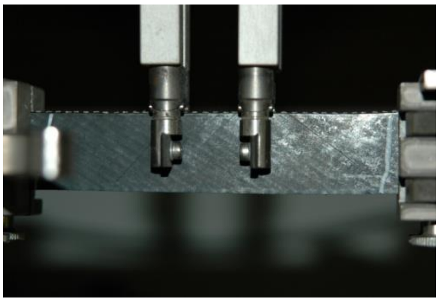

Fig. 3.1. Tension test of fibre composite with rubber matrix

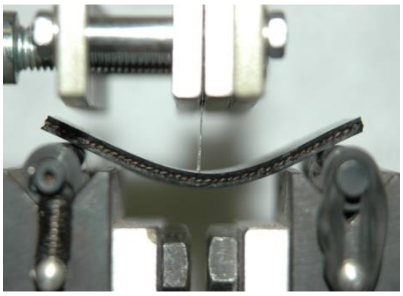

Fig. 3.2. Bending test of fibre composite with rubber matrix

Bending tests were realized also with the ZWICK testing machine as a three point bending. Also pure rubber specimens were tested. During the test each specimen was placed in the test preparation and pushed against its middle part (Fig. 3.2). The dependency between the force and the middle deflection was recorded.

3.2. Results of bending simulations

The figures below present results of bending tests and their simulations. The tests were carried out with three groups of three specimens each: for 45° and 90° declination of fibres and for pure rubber. The same material parameters were set as for the tension test simulations.

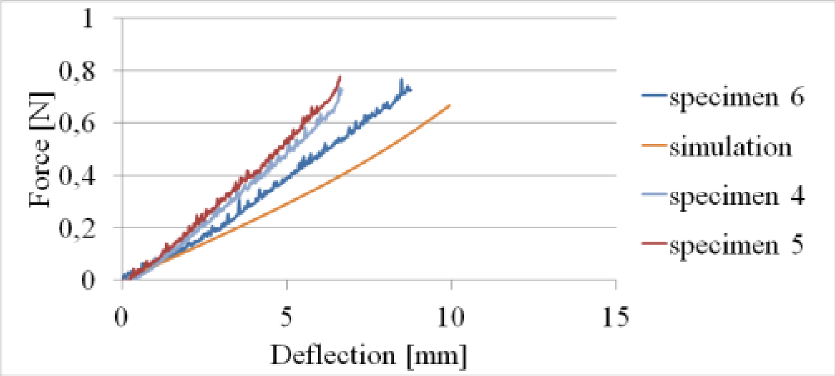

Fig. 3.6. Results of the bending test and its simulation for 45° declination of fibres.

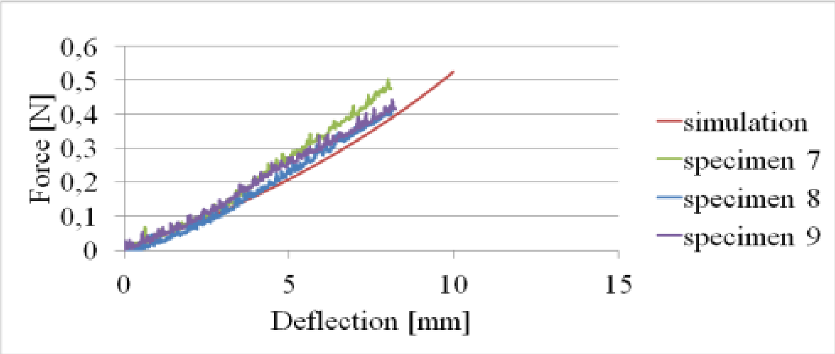

Fig. 3.7. Results of the bending test and its simulation for 90° declination of fibres.

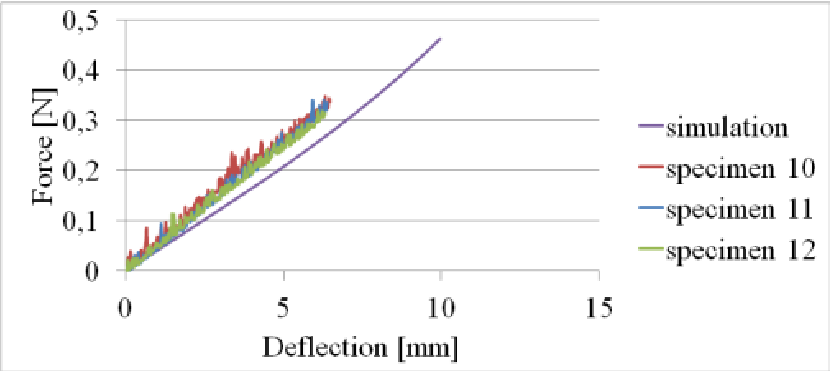

Fig. 3.8. Results of the bending test and its simulation. Specimens made of pure rubber.

As a result of the tests and simulations carried out it is verified that anisotropic hyperelastic constitutive model (in polynomial form) is able to simulate credibly results of tension and bending tests of fibre composites showing large strains under the following conditions: elastomer matrix shows negligible Mullins effect; bending stiffness of fibres is negligible. This result supports the earlier suggestion that in the case of not infinitely thin fibres the main reason of discrepancy between the unimaterial model and experiment lies in inability of the model to account for the bending stiffness and size effect of fibres.

4. Effective anisotropic constants within simplified mechanics of materials

In this section, the “rule of mixtures” approach is recapitulated for the approximate derivation of effective constants within the classic linear elastic mechanics. Then we proceed to apply a similar simplifying approach of mechanics of materials to include the additional parameter within the linear couple stress theory.

4.1. Effective properties of fibre composite within the linear elasticity

We review now the derivation of the effective material properties within the framework of linear elastic mechanics of materials. Specifically, long fibre composites are still considered. Assumptions and simplifications used in linear elastic mechanics of materials are employed. This approach sets the relationships between the effective properties and properties of the constituents. Engineering constants of an equivalent homogeneous material are derived using characteristics of the given composite and its components - volume fraction and geometric arrangement of fibres, matrix and fibre properties. Elementary models employ representative volume element (RVE) based on the following simplifications:

- RVE consists of fibre and matrix ;
- both fibre and matrix materials are linear elastic and isotropic;
- RVE geometry does not change in the 3rd direction;
- area fractions in the direction of fibres represent volume fractions;
- strains and stresses due to the Poisson’s ratio mismatch at the fibre-matrix interface are neglected;
- the actual fibre arrangement in space (hexagonal, tetragonal, random) is of no consequence;
- the round fibre is replaced with rectangular block with the same volume fraction;
- perfect bonding at fibre/matrix interface is assumed;
- cross-sections of both the matrix and fibre remain planar under any deformation;
- the composite is macroscopically homogeneous and transversally isotropic.

4.2. The inclusion of the fibre bending stiffness parameter

Generally the notation for couple stress components acting on the plane is as shown below:

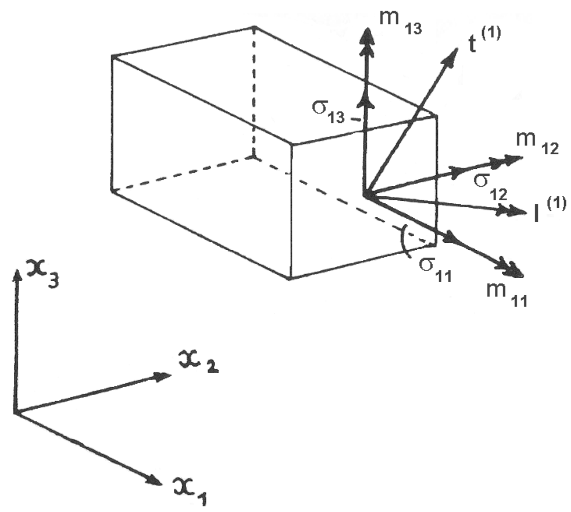

Fig. 4.1. RVE (a, b) [3]

But in this section only m_{13} is considered (plain strain problem for the unidirectional material). Presently, let us focus on a two-dimensional representative element of the composite. We consider the RVE consisting of a fibre element and matrix element; fibre is regarded as a simple beam; matrix material is assumed to be significantly softer. Such approach implies inextensibility of fibres, or the problem formulation in which fibre elongation is negligible.

Below we consider a general stress state of the composite. In **Fig. 4.2** below, the stress components acting on fibre and matrix elements represent an average of the actual stress distribution.

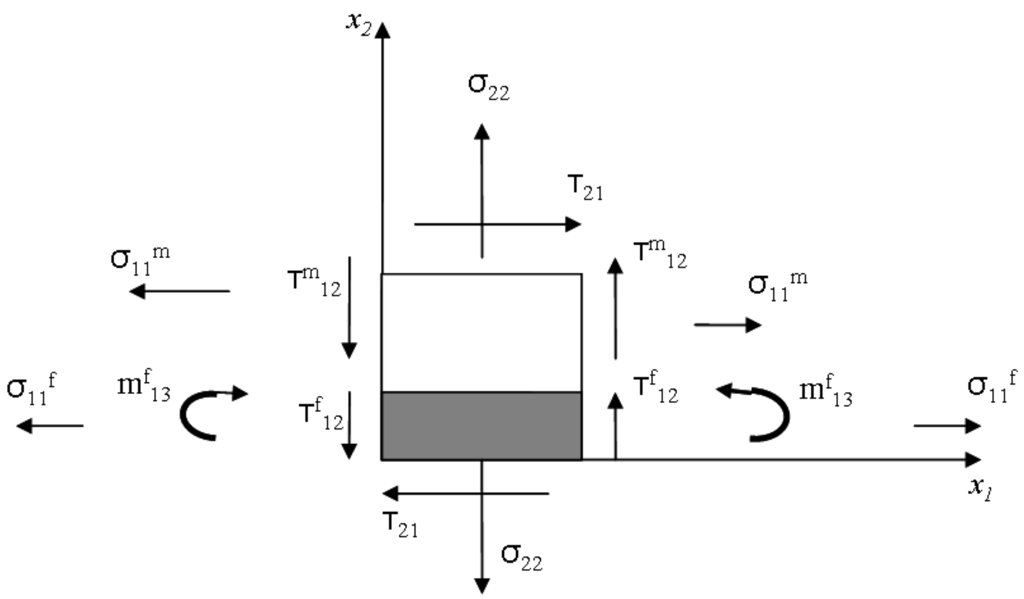

Fig. 4.2. RVE at a substructure scale: resultant loads for each constituent (matrix in the upper part and fibre in the lower part)

The actual stress distribution in the fibre cross-section (**Fig. 4.3**) is linked to the resultant loads in **Fig. 4.2** by averaging the function throughout the fibre element height.

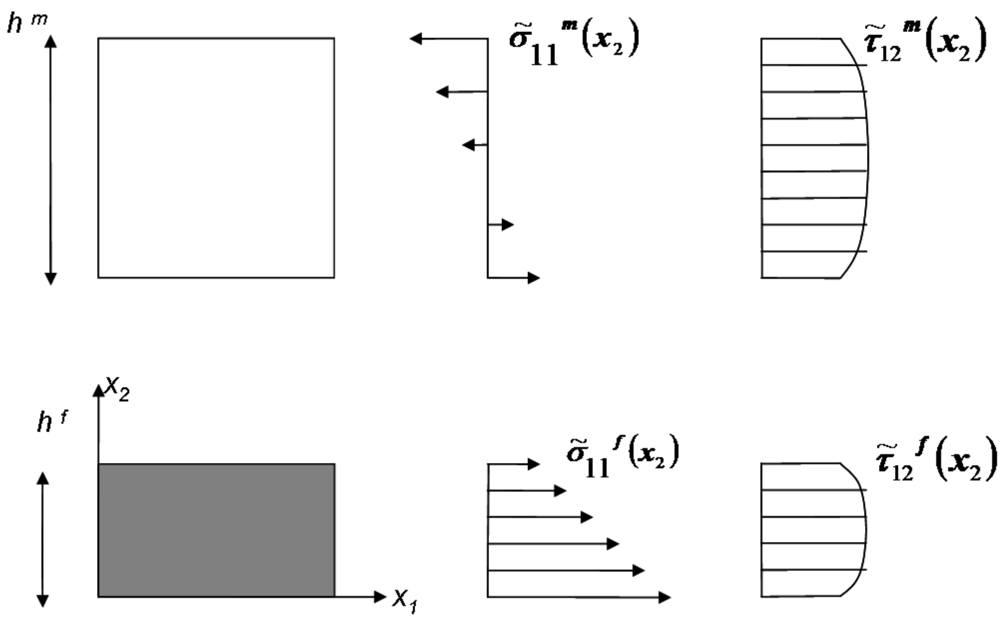

Fig. 4.3. Substructure scale: distributed load for the constituents

If we focus on the normal stress distribution $\tilde{\sigma}_{11}{}^f(x_2)$ acting in the fibre cross-section, we can see that it contains a constant part which corresponds to the resulting traction $\sigma_{11}{}^f$ and another linear part which corresponds to resulting couple stress $m_{13}{}^f$ (see **Fig. 4.4**)

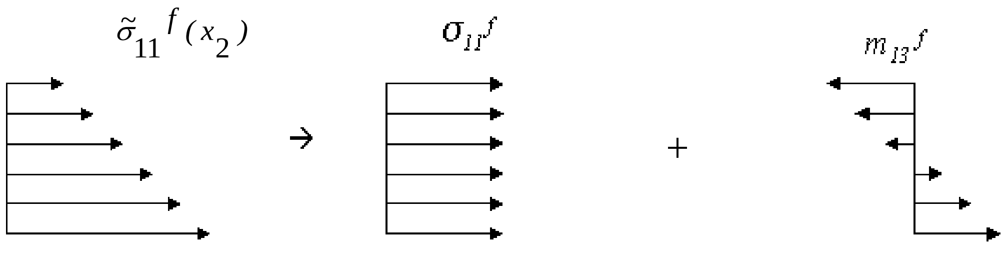

Fig. 4.4. The normal stress distribution and the resulting loads

Now we can transform the real stresses to the equivalent homogenised cell below (**Fig. 4.5**) (by averaging the function throughout the whole representative element hight ***h***):

$$m_{13} = \frac{1}{h}\left(\int_0^{h^f} \tilde{\sigma}_{11}{}^f x_2 dx_2 + \int_{h^f}^{h} \tilde{\sigma}_{11}{}^m x_2 dx_2 \right) \tag{4.28}$$

$$\tau_{12} = \frac{1}{h}\left(\int_0^{h^f} \tilde{\tau}_{12}{}^f dx_2 + \int_{h^f}^{h} \tilde{\tau}_{12}{}^m dx_2 \right) \tag{4.29}$$

$$\sigma_{11} = \frac{1}{h}\left(\int_0^{h^f} \tilde{\sigma}_{11}{}^f dx_2 + \int_{h^f}^{h} \tilde{\sigma}_{11}{}^m dx_2 \right) \tag{4.30}$$

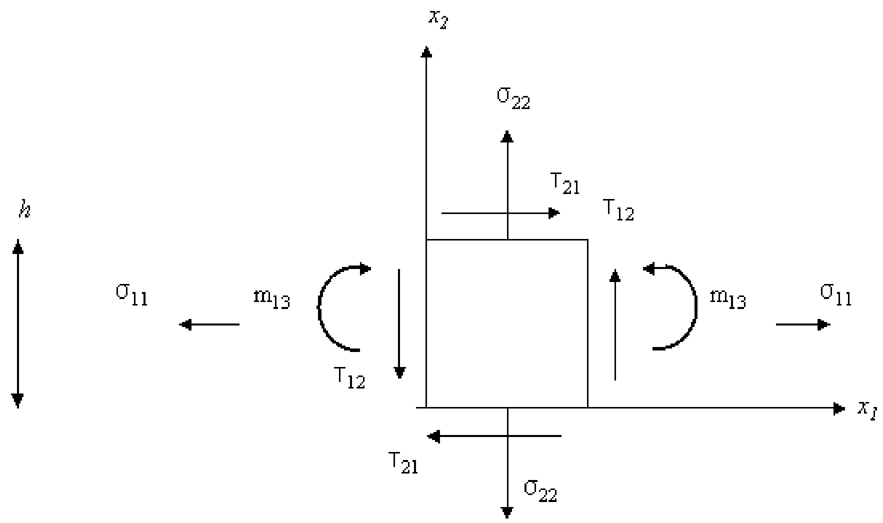

Fig. 4.5. EVE (macro-scale)

The equivalent strains can be obtained by averaging as well, similarly to the equivalent stresses depicted above. In a current desciption, we accept that on the substructure scale the fibres behave as simple beams; on a macro scale (**Fig. 4.5** above) when we consider an equivalent element of the homogenised continuum, the only independent degrees of freedom are displacements.

A more complicated model of the unit cell is used by Fleck and Shu in [30]. There the fibre element is modelled as Timoshenko beam experiencing both bending and shear deformation. Such behaviour on a substructure scale corresponds to the general Cosserat theory with presence of the additional degree of freedom - rotation in the point.

5. Composites reinforced with fibres resistant to bending: mathematical model for large strains and its implications

5.1. Introduction of the modified invariants and energy density function

To construct computationally applicable strain energy form suited for the rubber-like composites reinforced with stiff fibres, simplifying assumptions were employed by Lasota [3]. The strain energy density W was restricted to be at most quadratic function of the components of $\boldsymbol{\Lambda}$. Such assumption, as pointed out in [2], implies that the fibre radius of curvature is large compared to the substructure dimensions (fibre diameters or fibre spacing). To reduce the amount of invariants, the coupling between $\boldsymbol{\Lambda}$ and $\boldsymbol{C}$ is ignored. For simplicity the strain energy density function is chosen to contain only one additional invariant accounting for the bending stiffness of fibres.

Modified invariants can be introduced on the basis of modified tensors.

$$\bar{I}_1 = \bar{C}_{AA} = J^{-2/3} C_{AA}, \tag{5.1}$$

$$\bar{I}_4 = A_B \bar{C}_{CB} A_C = J^{-2/3} A_B C_{CB} A_C, \tag{5.2}$$

In the present work the form of the energy density is modified and the invariant $\bar{\boldsymbol{I}}_6$ is included:

$$\begin{aligned}\bar{I}_6 &= A_B \bar{\Lambda}_{OB} \bar{\Lambda}_{OC} A_C = J^{-4/3}\Big(A_B \Lambda_{OB} \Lambda_{OC} A_C - \\ &- \frac{1}{3} F^{-1}_{OK} G_{KO} A_L C_{LR} \Big(A_S \Lambda_{RS} F^{-1}_{OK} G_{KO} + A_N \Lambda_{RN} - \frac{1}{3} G_{BC} F^{-1}_{CB} A_O C_{OR} \Big)\Big),\end{aligned} \tag{5.3}$$

$$W = k_1\left(\bar{I}_1 - 3\right) + k_2\left(\bar{I}_4 - 1\right)^2 + k_3 \bar{I}_6 + \frac{1}{d}\left(J - 1\right)^2. \tag{5.4}$$

5.2. Parameter k_3 for the fibre reinforced incompressible material

We continue to consider a beam reinforced by parallel fibres subjected to pure bending with respect to X_2 axis. For simplicity, material incompressibility is assumed. Fibres are initially aligned along the X_1 direction, so vector $A=(1;0;0)^T$. In this case it holds for the energy density

$$W = \frac{\mu}{2}\left(I_1 - 3\right) + k_2\left(I_4 - 1\right)^2 + k_3 I_6 \tag{5.5}$$

where unmodified invariants I_1, I_4, I_6 can be used.

The constant k_3 is determined from the condition of equality of the bending stiffnesses of the homogeneous and heterogeneous models:

$$k_3 = \frac{3}{8} \frac{E_m J_m + E_f J_f - E_{hom} J}{S} \tag{5.6}$$

This formula is analogous to the rule of mixture in application to the bending stiffness. The effective bending stiffness of the initial heterogeneous model is "smeared out" uniformly throughout the section of the homogeneous model by means of the couple stress theory.

5.3. Numerical examples

The new finite element code developed in Matlab software by Lasota [3] is used below for computations within polar theory, and Ansys software is used for computations within conventional theory. The new code has been undergoing changes and modifications; the modifications introduced by me included:

- the change of the constitutive model and all the related finite element equations in accordance with (5.3, 5.4);
- reformulation of code equations in the matrix form instead of index form which reduced the computational time substantially.

As an illustrative example, let us consider a fibre reinforced thin rectangular plate with two rows of unidirectional fibres undergoing four-point bending (**Fig. 5.1**). As the fibre diameter is comparable to the dimensions of the specimen, size effect is to be expected. The given specimen is modelled in three different ways:

- via a heterogeneous FE model with explicitly modelled fibres embedded in matrix;
- via equivalent homogeneous transversally isotropic FE model in accordance with the classic elasticity (later referred to as classic model);
- via equivalent homogeneous transversally isotropic FE model in accordance with the couple stress theory (later referred to as CST model).

5.3.1. A thin composite plate with 0 degrees fibre declination: four-point bending

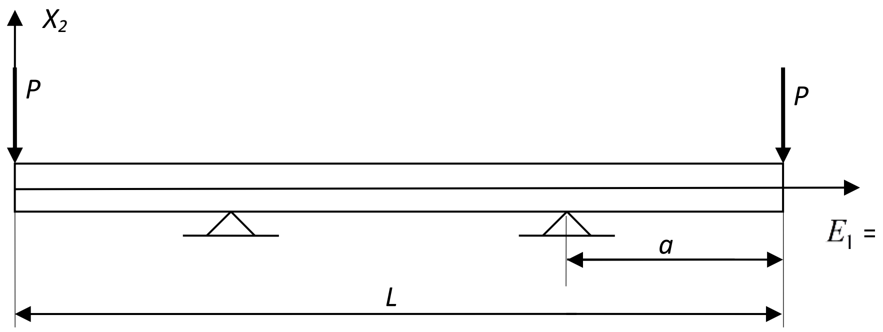

Fig. 5.1 Four-point bending

The classical model with fibre direction defined by vector $\boldsymbol{A}$ $(1,0,0)^{\mathrm{T}}$ is based on the strain energy density

$$W = \frac{\mu}{2}\left(I_1 - 3\right) + k_2\left(I_4 - 1\right) + \frac{1}{d}\left(J - 1\right)^2 \tag{5.7}$$

In the CST model a new term I_6 is added related to the curvature of the deformed fibres. The corresponding hyperelastic anisotropic potential is as follows:

$$W = \frac{\mu}{2}\left(\bar{I}_1 - 3\right) + k_2\left(\bar{I}_4 - 1\right)^2 + k_3\bar{I}_6 + \frac{1}{d}\left(J - 1\right)^2 \tag{5.8}$$

The objective of setting all the constants is to simulate correctly both tensile and bending behaviour of the given heterogeneous model. Results of all the three simulations are compared in **Fig. 5.2.**

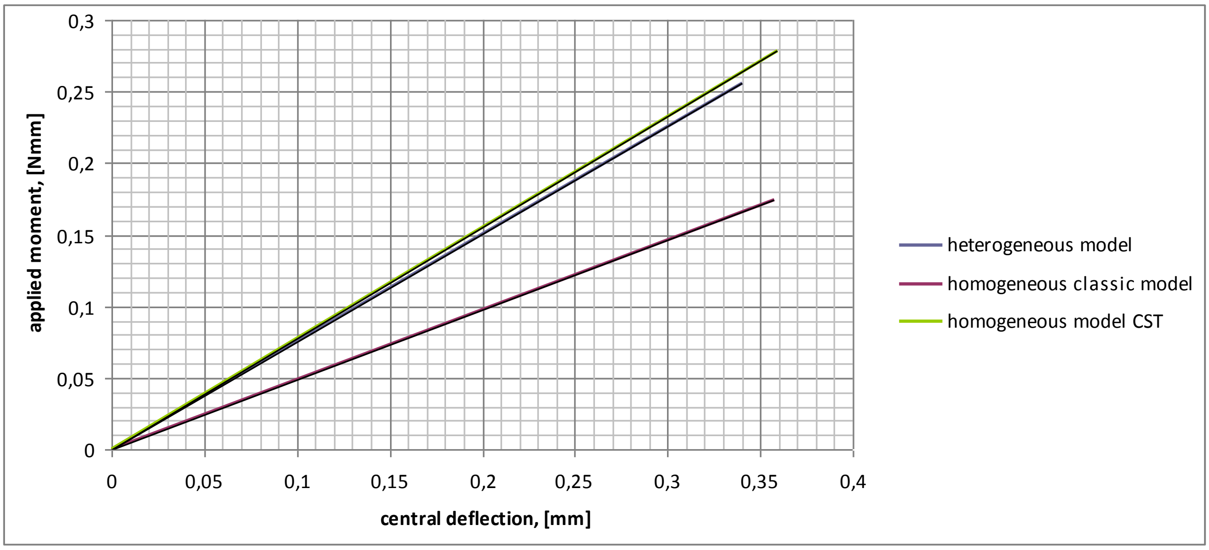

Fig. 5.2 Comparison of FE simulations of 4-point bending using different constitutive models.

5.3.2. A thin composite plate with 30 degrees fibre declination: four-point bending

The example above is a standard linear problem which can be solved analytically with respect to the deflection which can be assumed constant throughout the plate thickness. This simplicity occurs due to the fibres being aligned along the X_1 axis. In the present example, we consider the case when the fibres have 30 degrees declination angle which renders the problem unsolvable analytically. The plate is loaded as shown in **Fig. 5.1.** The constant k_3 is determined using (5.6) on the basis of the corresponding representative periodic element containing two fibres in the cross-section (**Fig. 5.3**).

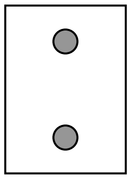

Fig. 5.3 Representative periodic element

The values of the material parameters are as follows: k_2 =*12.75 MPa*, k_3 =*-25.27 Pa·m*^{2}. Negative value of the constant k_3 indicates that the bending stiffness of the classical homogeneous model, generated by the averaged tensile stiffness of the heterogeneous plate, is higher than the actual plate's bending stiffness. So the CST model is constructed by augmenting the classic model with the additional term that, roughly speaking, subtracts the excessive bending stiffness without affecting the tensile properties of the model in any way (which are in complete agreement with the heterogeneous structure already).

Importantly, the fibre direction unit vector is now defined as $(0.866, 0, 0.5)^T$

Fig. 5.4. Comparison of FE simulations of 4-point bending using different constitutive models for the case of fibre declination angle of 30 degrees.

6. An exact solution of the boundary problem for the thick polar material plate for the linearized case

In this section, thick fibre-reinforced plate under certain boundary conditions is considered. Polar theory equations are employed in linear formulation. The solution of the plane strain boundary problem of polar elasticity for the static and dynamic flexure of a thick laminated plate has been recently derived by Farhat and Soldatos in [7]. The authors take into account the contribution of the couple stresses with the help of one extra elastic modulus. In the present study, after reproduction of the solution presented in [7] for the case of static flexure of a single-layer plate, the solution is extended to different boundary conditions with three extra elastic moduli in the model. In this chapter some new numerical results are presented which complement those in [7].

6.1. Problem setting

Let us consider a planar boundary problem: a thick transversely isotropic plate, infinite in the x_3 direction, subjected to certain boundary conditions corresponding to the plane strain. In this case, the displacements are functions of only two coordinates

$$\begin{aligned} u_1 &= u_1(x_1, x_2),\\ u_2 &= u_2(x_1, x_2),\\ u_3 &= 0. \end{aligned} \tag{6.1}$$

The following equations in terms of displacements u_1, u_2, obtained by Spencer and Soldatos [2] for the case of the plane strain problem of the plate with the fibres initially aligned with x_1 direction, will be further employed:

$$\begin{aligned} &c_{11}\frac{\partial^2 u_1}{\partial x_1^2} + (c_{12}+c_{66})\frac{\partial^2 u_2}{\partial x_1 \partial x_2} + c_{66}\frac{\partial^2 u_1}{\partial x_2^2} + c_2\frac{\partial^4 u_1}{\partial x_1^2 \partial x_2^2} + c_3\frac{\partial^4 u_2}{\partial x_1^3 \partial x_2} + c_1\frac{\partial^4 u_2}{\partial x_1 \partial x_2^3} = 0,\\ &c_{66}\frac{\partial^2 u_2}{\partial x_1^2} + (c_{12}+c_{66})\frac{\partial^2 u_1}{\partial x_1 \partial x_2} + c_{22}\frac{\partial^2 u_2}{\partial x_2^2} - c_1\frac{\partial^4 u_2}{\partial x_1^2 \partial x_2^2} - c_2\frac{\partial^4 u_1}{\partial x_1^3 \partial x_2} - c_3\frac{\partial^4 u_2}{\partial x_1^4} = 0. \end{aligned} \tag{6.2}$$

where c_{ii} represent stiffness matrix components from classic elasticity, and c_i are elastic moduli that characterise the substructure (c_1 , c_2 correspond to the resistance to “splay” mode deformation of fibres and c_3 - to “bending” mode deformation).

6.2. Solution

We make use of the method of the boundary problem solution in [7] for the case of static flexure of a single-layered plate and extend it to different boundary conditions (**Fig. 6.1**) and additional components of the model (terms with coefficients c_1, c_2 in the system (6.2)).

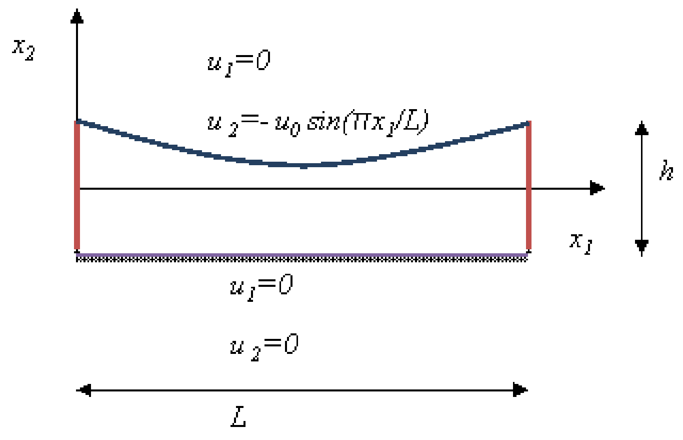

Fig. 6.1 Displacement boundary conditions

For a plate under the above specified load, the solution in the following form can be used:

$$u_1 = f_1(x_2)cos\left(\frac{\pi x_1}{L}\right),$$
$$u_2 = f_2(x_2)sin\left(\frac{\pi x_1}{L}\right) \tag{6.15}$$

where

$$f_1(x_2) = a_i e^{\mu_i x_2},$$
$$f_2(x_2) = \bar{a}_i e^{\mu_i x_2}. \tag{6.16}$$

6.3. Results

The elastic constants for the transversely isotropic material are set as follows: E_L =40 E_T , G_{LT} =0.5E_T , G_{TT} =0.2 E_T, ν_{TT} = ν_{LT} =0.25. Adopting notation from [7] we set

$$d_{31}=c_{11}\ \tilde{\lambda}\ hL \tag{6.17}$$

where $\tilde{\lambda}$ is a non-dimensional parameter related to intrinsic material length parameter (for more details see [7]). Each of the remaining moduli can be set in the similar manner ($d_{11}=c_{11}\tilde{\lambda}_1 hL$, $d_{33}=c_{11}\tilde{\lambda}_2 hL$), although the definition of these moduli is out of the scope of this study. For each calculation only one additional elastic modulus is considered nonzero, the other additional moduli are omitted from the model (i.e., not present in the system (6.10)). Thus a quantitative estimation of the influence of each of the additional elastic moduli is obtained.

7. APPLICATION OF POLAR ELASTICITY TO BENDING OF A THICK PLATE UNDER SMALL STRAINS.

To gain a better understanding of the additional constant and the role of couple stress in polar theory [2], we focus on exact analytical (polar elasticity) solutions for the problem of pure bending of thick infinite plates. The solution is done for a transversely isotropic material under small strain assumption.

7.1. Comparison summary

To briefly illustrate the differences in the equivalent models, a summary of the is presented below for comparison.

classical (EC) periodic (PS) couple stress (EP)

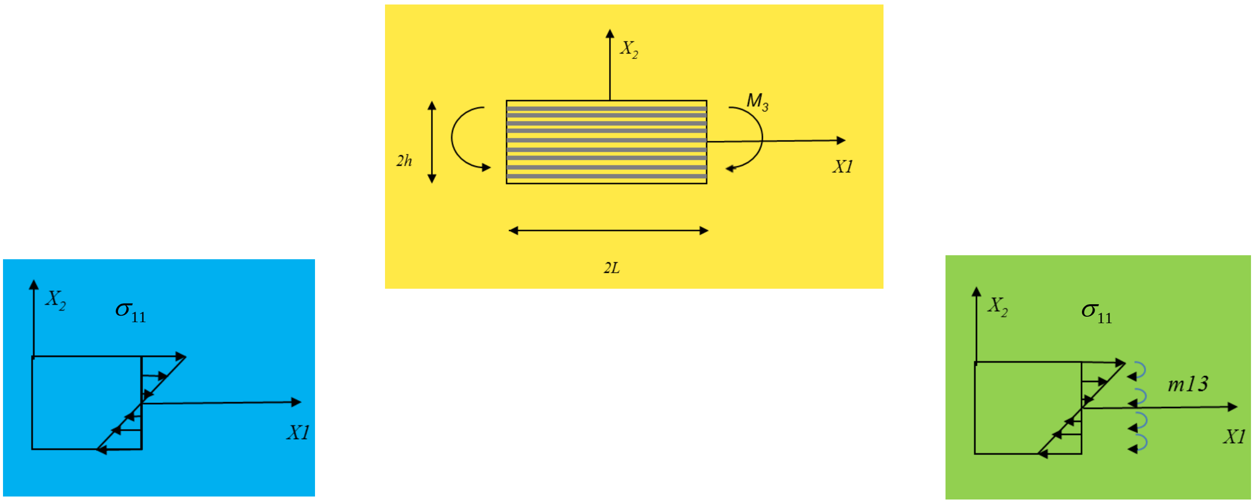

$$\int_{-h}^{h} \sigma_{11} x_2 dx_2 = M_3$$

$$\int_{-h}^{h} \sigma_{11} x_2 dx_2 + \int_{-h}^{h} m_{13} dx_2 = M_3$$

Fig. 7.1. Comparison of the models. Bending moment

The heterogeneous plate (PS model) under pure bending can be modelled as effective classic (EC) homogenous model (option 1) or effective polar (EP) homogeneous model (option 2). The overall applied bending moment in all the cases has the same value, but the stress distribution is different. In the 1st model the moment is transferred to the material by tensile stress only, and in the 2nd model the moment is transferred by tensile stress as well as couple stress. While normal stress is related to the extension or compression of the fibre, Couple stress is directly related to the fibre curvature only.

In order to compare the above 3 models, the equivalent effective material parameters must be defined. We start with the heterogeneous (periodic) model: E_1 is the function of x_2, the rest of parameters are constants. Its periodically changing stiffness can be regarded as an approximation of the fibre reinforced composite.

For the EC homogeneous model the E_1 is defined by averaging, and the rest of the constants are the same.

For the EP homogeneous model, all the constants are identical to the classic, but the additional parameter is present. Bending stiffness parameter d_{31} serves as a correction parameter which ensures that the overall bending stiffness of the plate in the EP model equals that one of the PS model.

Even without going into detail, we can see that characteristics of the heterogeneous model are more comprehensively accounted for in the second (EP) model: particularly, the amplitude E wave is not present in the 1st model in any way, since it has no effect on the averaged modulus. Also the number N which is indicative of the number of fibres can not be included in the 1st model.

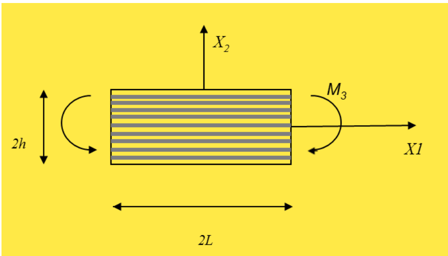

$$E_1 = E_0 + \tilde{E}\cos\left(\frac{\pi N}{h} x_2\right),$$

E_2, ν_{12}, ν_2, G_{21}.

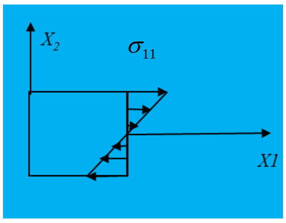

$E_1 = E_0$

E_2, ν_{12}, ν_2, G_{21}.

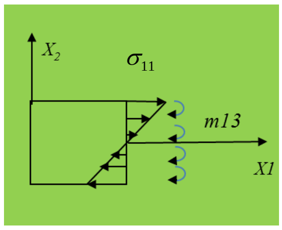

$E_1 = E_0$

E_2, ν_{12}, ν_2, G_{21}.

$$d_{31} = \frac{2h^2 \tilde{E}}{\pi^2 N^2 (1 - \nu_{21}\nu_{12})}$$

Fig. 7.2. Comparison of the models. Material parameters

8. Verification of the FEM code based on the exact solutions for small strain problems

Verification is carried out using new exact solutions for the anisotropic couple stress continuum with the incompressibility constraint. Considerations and techniques employed in Section 6 are used to achieve exact solutions of the linear boundary problems below. Plane strain boundary problem is solved both analytically and numerically (using the new FEM code). The large strain problem is also examined.

8.1. Choice of the specific form of the model – incompressible material

The strain energy density is modified for material incompressibility:

$$W = k_1(I_1 - 3) + k_2(I_4 - 1)^2 + k_3 I_6 + p(J - 1) \tag{8.1}$$

where p is Lagrange multiplier related to incompressibility and J is the volume ratio. The coefficients in eq. (8.1) represent material parameters: k_1 is related to properties of the matrix, k_2 and k_3 relate to the tensile and bending stiffness in the direction of reinforcement, respectively.

8.2. Results

The solver by Lasota [3] is based on finite element method (FEM) and applies the polar (couple stress) theory. To test the applicability of this solver, it is applied to two plane strain problems in the first part of this section. In order to verify the element formulation and the chosen form of strain energy density function, the FEM numerical results are compared with values obtained analytically. Since there are no analytical solutions available for large strain anisotropic polar elasticity, we consider a small strain case here.

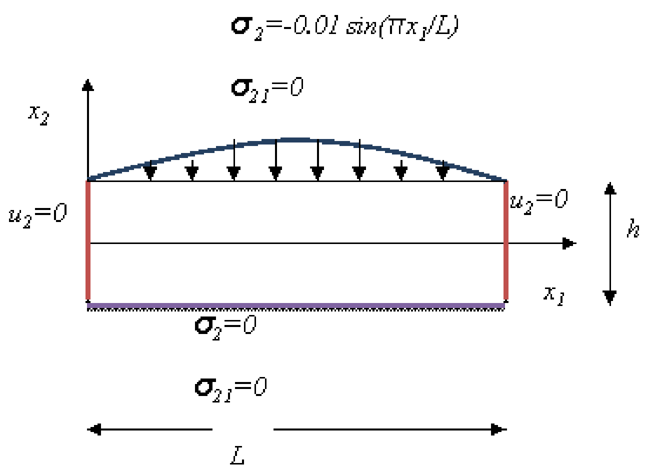

Fig. 8.1. Boundary value problem

Analytical solution of a plane strain boundary problem of polar elasticity for flexure of the thick plate under sinusoidal pressure load (**Fig. 8.1**) has been derived recently by Farhat and Soldatos in [7]. Complete boundary conditions are depicted in **Fig. 8.1**.

Numerical and analytical results for the normal stress and the couple stress along the axis x_2 (in the cross-section $x_1=L/2$) are depicted in **Figs. 8.2, 8.3**, respectively. All the FEM results show highly accurate agreement with the exact analytical curves.

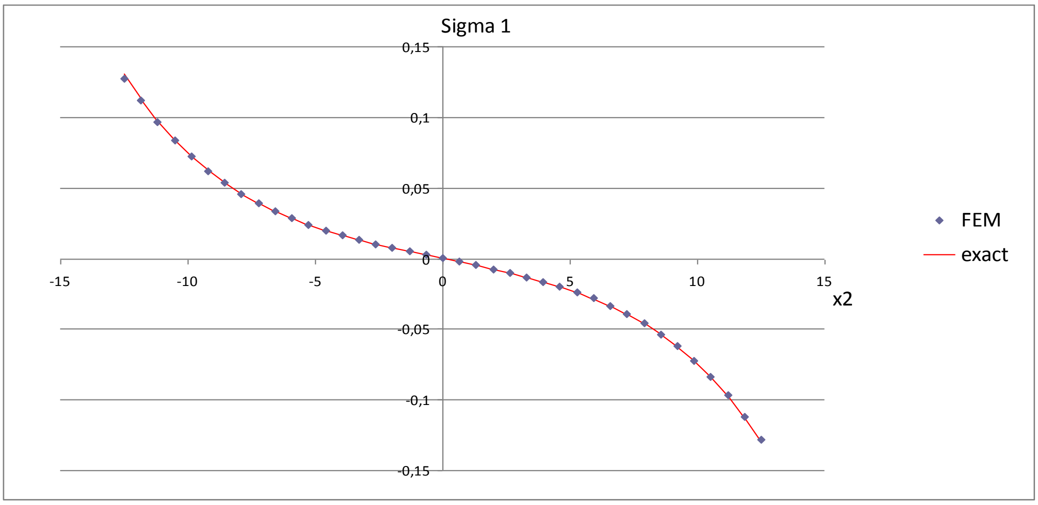

Fig. 8.2. Distribution of first principal stress σ_1 throughout the thickness of the plate in the middle section (x_1=L/2).

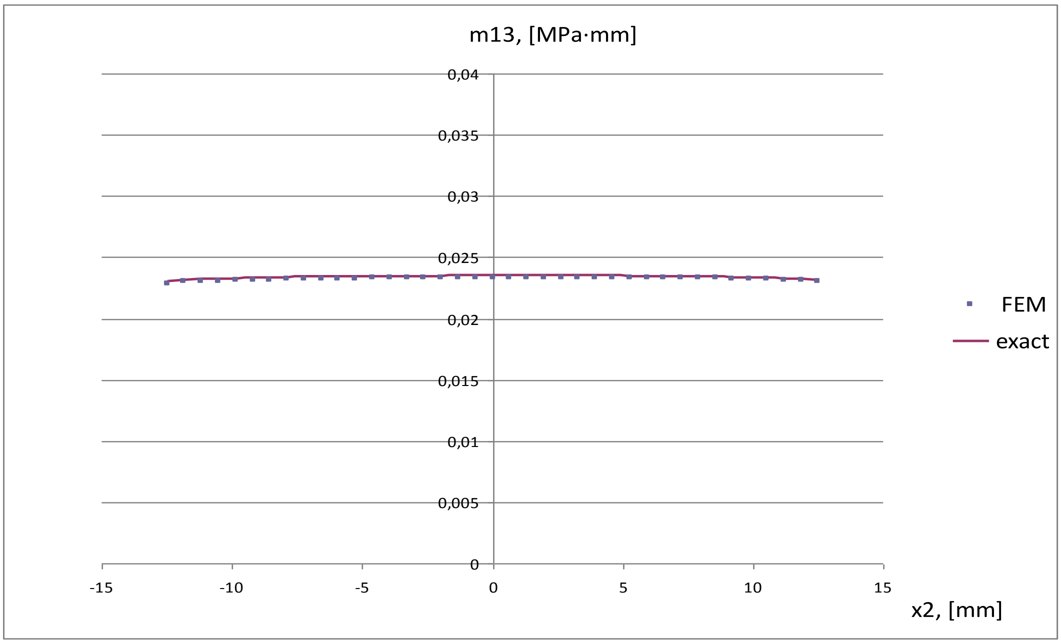

Fig. 8.3. Distribution of couple stress m_{13} throughout the thickness of the plate in the middle section (x_1=L/2).

Also, to illustrate the capability of the FEM code to solve problems under large strains, tension test of a fibre reinforced elastomer specimen loaded in another direction than that of the fibres was simulated (**Fig. 8.4**). The FEM applications on the basis of both classical elasticity and nonlinear polar theory are compared (**Fig. 8.5, Fig. 8.6**).. As expected, the non-zero parameter k_3 influences the response by adding anisotropic bending stiffness to the model (namely, to the implicitly present fibres).

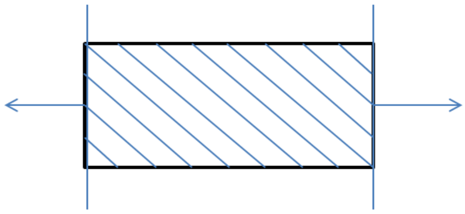

Fig. 8.4. Specimen of fibre reinforced elastomer loaded in tension

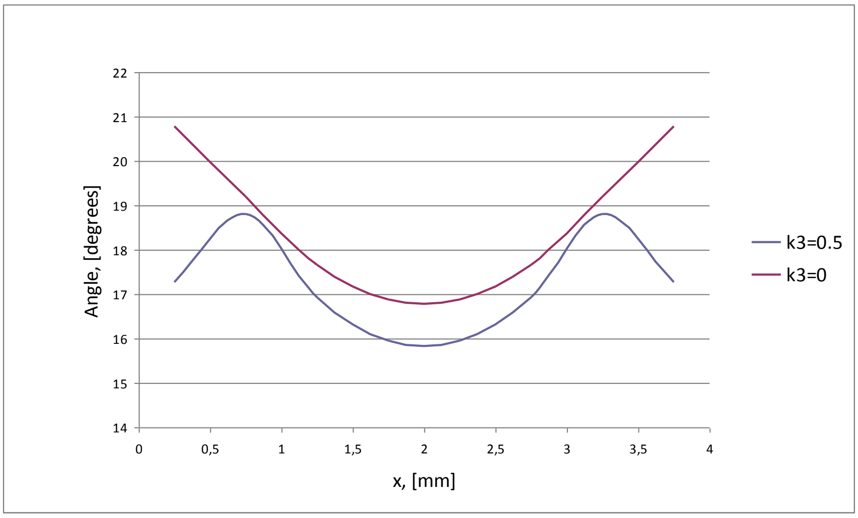

Fig. 8.5. Comparison of the deformed fibre rotation angle in both models under the same load

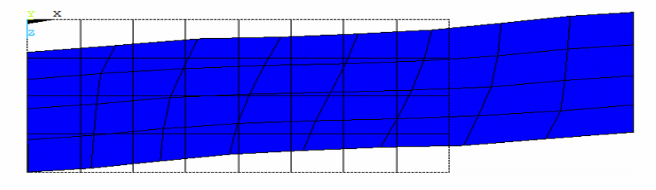

Fig. 8.6. Deformed and undeformed mesh of the fibre reinforced elastomer under tension (k_3=0.5)

In the large strain range no solution enabling us a verification was found in literature, so the presented example illustrates only qualitatively the capability of the code to mimic the bending stiffness of the fibres. When the parameter k_3 is set to zero in the applied material model, it is reduced to a classical (Cauchy) model taking only tension stiffness of the fibres into consideration, i.e. based on the assumption of the infinitesimal diameter of fibres and their uniform distribution.. Addition of a non-zero value of the k_3 parameter has increased the stiffness of the specimen, demonstrating thus the increased resistance of the specimen against deformation caused by bending stiffness of the fibres.

9. Problems with kinematic constraints: linear elasticity with and without additional bending stiffness

9.1. Problem setting

Let us consider a plane strain boundary problem: a simply supported thick transversely isotropic plate, infinite in the x_3 direction, loaded by sinusoidal pressure on the top surface. In this case, the displacements are functions of only two coordinates x_1, x_2. The material in question is transversely isotropic with high tensile stiffness in x_1 direction. It simulates a fibre-reinforced composite with one family of straight fibres. Boundary conditions include sinusoidal pressure on the top surface of the plate and zero vertical displacement at the ends of the plate, similar to **Fig. 8.1**.

9.2. Incompressibility constraint case

Here the focus is on the incompressible material and corresponding elastic solutions. The constitutive relations in the following general form [41] for symmetric stress components are

$$\sigma_{(ij)} = \lambda\theta\delta_{ij} + 2\mu_T\varepsilon_{ij} + \alpha\left(\varepsilon_{11}\delta_{ij} + \theta a_i a_j\right) + \beta\varepsilon_{11}a_i a_j + 2\left(\mu_1 - \mu_T\right)\left(a_i\varepsilon_{j1} + a_j\varepsilon_{i1}\right), \quad (9.1)$$

where $\theta = \varepsilon_1 + \varepsilon_2 + \varepsilon_3$. We use $\lambda -> \infty$ (which corresponds to incompressibility), and α is not present in the relations after simplifying. The second part of the constitutive equations is:

$$m_{13} = d_{31}\frac{\partial^2 u_2}{\partial x_1{}^2} \quad (9.2)$$

With regard to material incompressibility we use hydrostatic pressure $P = -\frac{1}{3}(\sigma_1 + \sigma_2 + \sigma_3)$. Thus, three independent material constants μ_{1T}, μ_T. β are required for the description of a transversely isotropic incompressible material, and four constants (with d_{31}) if the fibre bending stiffness is included in formulation. The solution is sought in the form

$$\begin{aligned} u_1 &= \bar{c}_i e^{\mu_i x_2} \cos\left(\frac{\pi x_1}{L}\right), \\ u_2 &= c_i e^{\mu_i x_2} \sin\left(\frac{\pi x_1}{L}\right), \\ P &= \tilde{c}_i e^{\mu_i x_2} \sin\left(\frac{\pi x_1}{L}\right). \end{aligned} \quad (9.3)$$

This corresponds to the boundary conditions applied at the plate ends. The upper and lower boundary conditions for the present problem, i.e. along the upper and lower surfaces, are set as follows:

$$\begin{cases} \sigma_{21}(x_1, h/2) = 0, \\ \sigma_2(x_1, h/2) = -q_0 \sin(\pi x_1 / L), \\ \sigma_2(x_1, -h/2) = 0, \\ \sigma_{21}(x_1, -h/2) = 0. \end{cases} \tag{9.4}$$

The present (extensible) incompressible formulation is further referred to as EIF (with hydrostatic pressure as additional unknown and kinematic constraint employed) and a "general" (extensible and compressible) material formulation is further referred to as GF. We approach EIF with GF by setting respective material constants closer to the values corresponding to incompressibility. In terms of generalised Hooke's law for transversely isotropic material, perfect incompressibility is achieved by setting Poisson's ratios as follows:

$$\begin{cases} \nu_{1T} = 0.5 \\ \nu_{T1} + \nu_T = 1 \end{cases} \tag{9.5a, b}$$

9.3. Inextensibility constraint case

In this section the material in question is set to be inextensible in x_1 direction (this represents inextensible fibres). The constitutive description involves Lagrange multiplier T which is related to unknown tension in x_1 direction. Applying the corresponding constitutive equations for the present plane strain problem we obtain:

$$\begin{aligned} \sigma_{11} &= \lambda \varepsilon_2 + T \\ \sigma_{22} &= (\lambda + 2\mu_T)\varepsilon_2 \\ \sigma_{(12)} &= 2\mu_{1T}\varepsilon_{12} \end{aligned} \tag{9.6}$$

Similarly to (9.4) the solution is chosen as follows:

$$\begin{aligned} &u_1 = 0, \\ &u_2 = c_i e^{\mu_i x_2} \sin\left(\frac{\pi x_1}{L}\right), \\ &T = \zeta_i e^{\mu_i x_2} \sin\left(\frac{\pi x_1}{L}\right) \end{aligned} \tag{9.7}$$

which corresponds to the boundary conditions applied at the plate ends.

The the upper and lower boundary conditions are given by:

$$\begin{cases} \sigma_{22}(x_1, h/2) = -q_0 \sin(\pi x_1 / L), \\ \sigma_{22}(x_1, -h/2) = 0, \end{cases} \tag{9.8}$$

The couple stress is

$$m_{13} = \left(\frac{\pi}{L}\right)^2 d_{31} c_i e^{\mu_i x_2} \sin\left(\frac{\pi x_1}{L}\right) . \quad (9.9)$$

Such formulation will be referred as EIF (extensible incompressible formulation). Thus, three independent material constants μ_{1T}, μ_T. λ are required (four if $d_{31} \neq 0$).

9.4. Inextensibility and incompressibility: double kinematic constraint

In this section, the material is assumed to be both incompressible and inextensible. The corresponding relations in the case of plane strain are:

$$\begin{aligned}
&\sigma_{11} = -P + T, \\
&\sigma_{22} = -P, \\
&\sigma_{(12)} = 2\mu_{1T}\varepsilon_{12} = \mu_{1T}\frac{\partial u_2}{\partial x_1} \\
&m_{13} = \left(\frac{\pi}{L}\right)^2 d_{31} c_1 \sin\left(\frac{\pi x_1}{L}\right)
\end{aligned} \quad (9.10)$$

Solution is sought in the form

$$\begin{aligned}
&u_1 = 0, \\
&u_2 = c \sin\left(\frac{\pi x_1}{L}\right), \\
&P = \left(\left(-\left(\frac{\pi}{L}\right)^2 \mu_{1T} - \frac{1}{2} d_{31}\left(\frac{\pi}{L}\right)^4\right) c_1 x_2 + c_2\right) \sin\left(\frac{\pi x_1}{L}\right), \\
&T = \left(\left(-\left(\frac{\pi}{L}\right)^2 \mu_{1T} - \frac{1}{2} d_{31}\left(\frac{\pi}{L}\right)^4\right) c_1 x_2 + c_2\right) \sin\left(\frac{\pi x_1}{L}\right),
\end{aligned} \quad (9.11)$$

The upper and lower boundary conditions are given by (9.8).

The formulation is here and further abbreviated as IIF (inextensible, incompressible formulation).

9.5. Effect of additional bending stiffness for inextensible incompressible material

The results obtained for the models in different formulations are compared with converging their effective properties. The convergence is established for the classical material description (d_{31}=0). In this paragraph the focus is on the resulting couple stress distribution in the middle cross-section of the plate. The d_{31} parameter is set the same in all computations. Different combinations of kinematic constraints and their effect on the couple stress distribution m_{13} are examined below.

The graph in (**Fig. 9.1**) illustrates convergence of the results obtained with general formulation (GF) to the result obtained with (extensible) incompressible formulation (EIF). For both d_{31}=10 N. We converge GF model to EIF by approaching Poisson ratio $\nu_{1T} \to 0.5$.

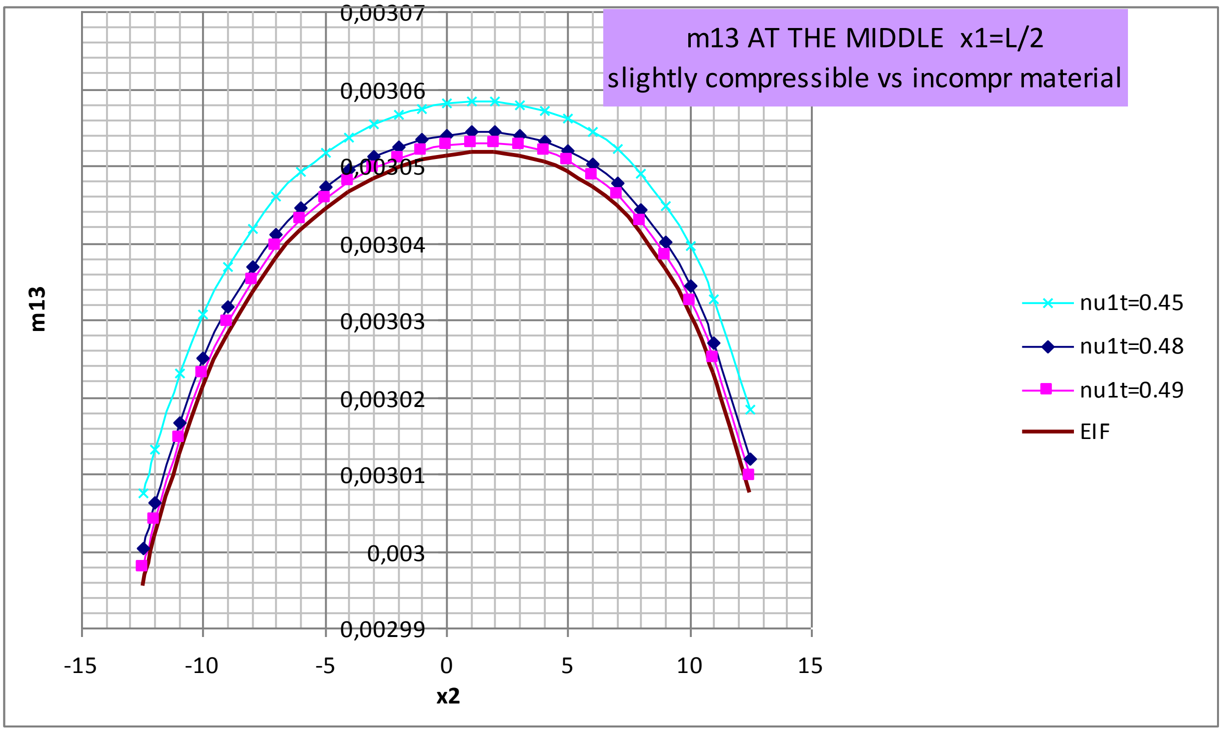

Fig. 9.1. Couple stress at the end of the plate calculated for different constitutive models

The comparison in **Fig. 9.2** is between two models (for both d_{31}=10 N) which we refer to as IIF (inextensible incompressible formulation) and EIF (extensible incompressible formulation) accordingly. The material properties were set such that EIF approaches inextensibility (E_1 is increasing).

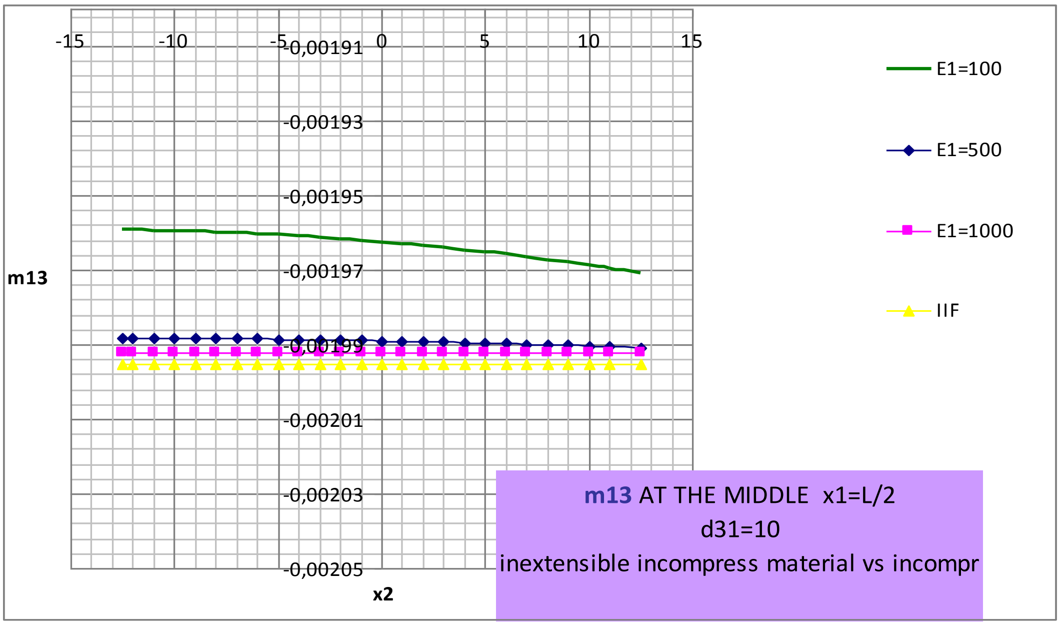

Fig. 9.2. Couple stress in the middle of the plate calculated for different constitutive models

As it can be seen from the figure below, with increasing longitudinal Young's modulus in EIF $E_1 \uparrow$, the couple stress m_{13} tends to constant value throughout the cross-section, as it is for IIF. Comparison in the **Fig. 9.3.** is between IIF model and inextensible (ICF) model. Relations that are valid for the inextensible (ICF) model:

$$\begin{cases} E_1 \to \infty \\ \nu_{T1} = \nu_{1T}\dfrac{E_T}{E_1} = 0 \end{cases} \tag{9.12}$$

In order to converge ICF to IIF, we take incompressibility relation (9.45b) and approach it by varying the parameter ν_T: $\nu_T \to (1 - \nu_{T1})$, so $\nu_T \to 1$

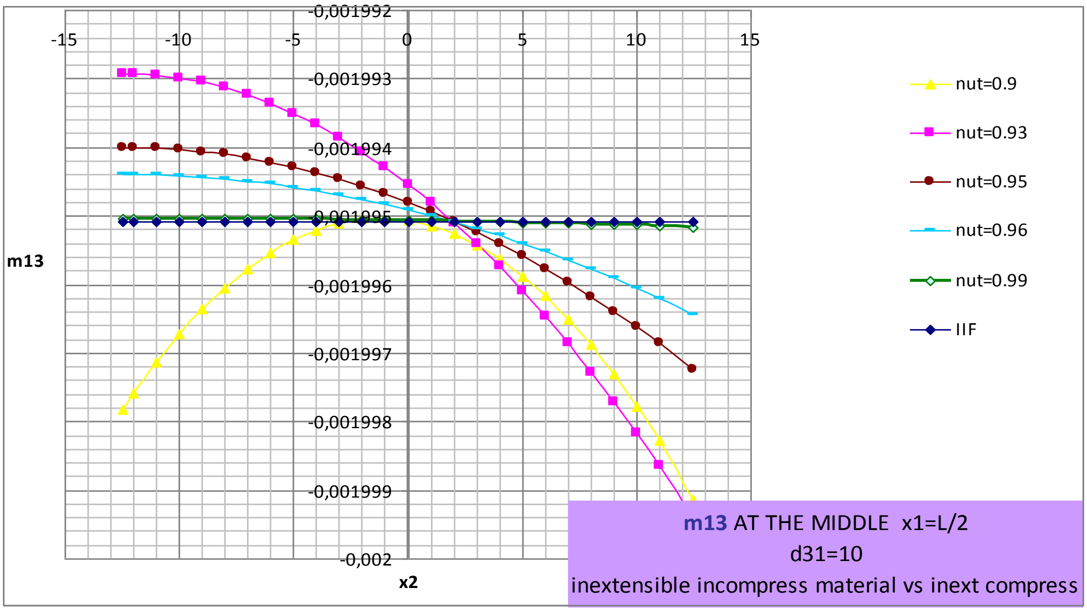

Fig. 9.3. Couple stress in the middle of the plate calculated for different constitutive models

9.6. Polar theory graphs examination

- EIF model (incompressible material with extensible, though stiff fibres) shows couple stress distribution close to constant in the cross-section. **Fig. 9.1** shows gradual convergence of the GF (general formulation) model results to the EIF ones.
- **Figs. 9.2, 9.3** show gradual convergence of the EIF and ICF results to IIF result (which is constant couple-stress distribution)
- Inextensible (ICF) model response converges to IIF by manipulating Poisson's ratio ν_T.
- Extensible incompressible (EIF) model response converges to IIF by increasing of Young/s modulus E_1.

10. CONCLUSIONS AND FUTURE WORK SUGGESTIONS

The current work is an attempt of a systematic study of the so called "polar elasticity for fibre-reinforced solids", its mechanical interpretation and specifics of numerical implementation and represents a natural continuation of Lasota's dissertation [3]. The contribution of fibres to the material stiffness is characterized by the tensile stiffness parameter and the additional parameters related to another fibre deformation mode (the focus of current work is bending mode of deformation).

The work starts with an experimental mechanical study with the steel fibre-reinforced rubber specimens. The fibres are comparatively thick and located in the middle plane of the specimen. The study shows the validity of the anisotropic unimaterial constitutive model in case of tension tests but its inability to simulate the bending behaviour of the composite correctly. This result supports the earlier suggestion that main reason of discrepancy lies in the inability of the model to account for the bending stiffness contribution and size effect of fibres.

As a next step, the general logic of the effective constants derivation is considered for a small strains case of fibre composites. The "rule of mixtures" approach of mechanics of composite materials is recapitulated, and a similar simplifying scheme is employed to include the additional parameter corresponding to the bending stiffness contributed by fibres.

The role of the additional effective constant in the model is investigated further on. The constitutive equations published in Spencer and Soldatos [2] are used to formulate a specific form of strain energy density function on the basis of constraint Cosserat theory (in which couple stresses are introduced and displacements or displacement rates are the only independent unknowns). This approach leads to second derivatives of displacement rates occurring in the finite element formulations. A specific form of strain energy density is proposed with an additional term correcting the effective bending stiffness of the continuum. The model used recently by Lasota [3] is examined and modified in order to make it more mechanically representative. For the modified constitutive model the issue of determination of the additional constant k_3 (associated with the fibre bending stiffness) is considered. Within the small strains framework, the formula is offered linking k_3 to the geometric and material properties of the initial heterogeneous structure.

The finite element code by Lasota [3] is modified to incorporate the additional invariant. Code equations are reformulated in the matrix form instead of index form which reduces the computational time substantially. The corresponding calculation is carried out for the composite plate under bending in the case of small strains. Two examples are considered: composite plate with fibres aligned along the longitudinal axis, and composite plate with fibres aligned under the angle of 30 degrees to the longitudinal axis. It is shown that the discrepancy between the classical homogeneous model and a heterogeneous model can be largely diminished by the presented approach.

A complementary study is also carried out for a thick fibre-reinforced plate under displacement boundary conditions. Polar elasticity equations are employed in linear formulation. The solution of the plane strain boundary problem of polar elasticity for the static and dynamic flexure of a thick laminated plate has been recently derived by Farhat and Soldatos [7]. The authors take the contribution of the couple stresses into account with the help of one extra modulus of elasticity. In the present study, after having reproduced the solution in [7] for the case of static flexure of a single-layer plate, I extended the solution to different boundary conditions with three extra modules of elasticity applied in the model. In this chapter some new numerical results are presented which complement those in [7].

In Section 7 a new pure bending elasticity solution is derived for the transversely isotropic polar material. It is compared with solutions based on the conventional theory in order to demonstrate how the size effect can be taken into consideration in the homogeneous polar model.

In Section 8 verification of the new constitutive model and finite element code [8] is carried out using new exact solution for the anisotropic couple stress continuum with the incompressibility constraint. Considerations and techniques employed in Section 6 are used to achieve exact solution of the linear boundary problem. Plane strain boundary problem is solved both analytically and numerically. The finite element calculations and analytical solution show perfect agreement. The large strain problem is also examined. In the large strain range no solution enabling us a comparison was found in literature, so the presented example illustrates only qualitatively the capability of the code to mimic the bending stiffness of the fibres.

In Section 9, a known linear elasticity problem is considered in two new ways. Firstly, constraints of incompressibility and inextensibility in fibre direction are added; secondly, the intrinsic anisotropic bending stiffness (based on polar elasticity) is included in the model. Inextensibility and incompressibility constraints cause the presence of respective Lagrange multipliers in the formulation. The resulting stress fields are compared to those obtained using the slightly compressible and slightly extensible formulation. The observed characteristics of stress distribution are compared and it is shown that those obtained with compressible and extensible formulations tend to the incompressible and inextensible ones with decreasing compressibility and extensibility. The scheme of determination of the additional constant d_{31} is suggested.

11. REFERENCES

[1] England AH (1999) Finite elastic deformations of a tyre modelled as an ideal fibre-reinforced shell. *J Elasticity* 54: 43-71

[2] Spencer AJM, Soldatos KP (2007) Finite deformations of fibre-reinforced elastic solid with fibre bending stiffness. *Int J Nonlinear Mech* 42:355-368

[3] Lasota T (2013) *Computational modelling of mechanical behaviour of "elastomer – steel fibre" composite.* Dissertation, Brno University of Technology

[4] Lasota T, Burša J, Fedorova S (2012) Constitutive equations and finite element formulation for anisotropic hyperelastic composites based on constrained Cosserat continuum. *ECCOMAS 2012 – European Congress on Computational Methods in Applied Sciences and Engineering*, e-Book full papers: 3379-3389

[5] Fedorova S, Lasota T, Burša J, Skácel P (2012) Experimental verification of a constitutive model of fibre composite with hyperelastic matrix. *Proceedings of Conference EAN 2012*, Tabor, CZ

[6] Soldatos KP (2013) Foundation of polar linear elasticity for fibre-reinforced materials. *J Elasticity* 114(2):155-178

[7] Farhat AF, Soldatos KP (2015) Cylindrical bending and vibration of polar material laminates. *Mech Adv Mater Struct* 22:885-896

[8] Fedorova S, Lasota T, Burša J (2016) Computational modelling of fibre composites with thick fibres as homogeneous structures with use of couple stress theory. In: Marcal PV, Yamagata N (Eds.), Design and Analysis of Reinforced Fiber Composites, *Proceedings of Symposium at WCCM XI - ECCM V - ECFD VI, Barcelona 2014* :25-48. ISBN 978-3-319-20006-4

[9] Lasota T, Burša J (2011) Simulation of mechanical tests of composite material using anisotropic hyperelastic constitutive models. *Eng Mech* 18(1): 23-32

[10] Spencer AJM (1972) *Deformations of Fibre-reinforced Materials*. Oxford University Press, London

[11] Demiray H (1972) A note on the elasticity of soft biological tissues. *J Biomech* 5:309-311

[12] Rachev A, Hayashi K (1999) Theoretical study of the effects of vascular smooth muscle contraction on strain and stress distributions in arteries. *Ann Biomed Engr* 27:459-468

[13] Zulliger MA, Rachev A, Stergiopulos N (2004) A constitutive formulation of arterial mechanics including vascular smooth muscle tone. *Am J Physiol Heart Circ Physiol* 287:H1335-H1343

[14] Klosner JM, Segal A (1969) Mechanical characterization of a natural rubber. *PIBAL Report* 6942 Polytechnic Inst. Brooklyn, NY

[15] Weiss JA, Maker BN, Govindjee S (1996) Finite element implementation of incompressible, transversely isotropic hyperelasticity. *Comput Meth Appl Mech Engrg* 135:107-128

[16] Ruter M, Stein E (1999) Analysis, finite element computation and error estimation in transversal isotopic nearly incompressible finite elasticity. *Comput Meth Appl Mech Engrg* 190:519-541

[17] Bonet J, Burton AJ (1998) A simple orthotropic, transversely isotropic hyperelastic constitutive equation for large strain computations. *Comput Meth Appl Mech Engrg* 162:151-164

[18] Reese S, Raible T, Wriggers P (2001) Finite element modelling of orthotropic material behaviour in pneumatic membranes. *Int J Solids Struct* 38:9525–9544

[19] Horgan CO, Saccomandi G (2005) A new constitutive theory for fiber-reinforced incompressible nonlinearly elastic solids. *J Mech Phys Solids* 53:1985–2015

[20] Nam TH, Marvalova B (2004) Deformation analysis of inflated cylindrical membrane of composite with rubber matrix reinforced by cords. *XXI International Congress of theoretical and applied mechanics ICTAM*

[21] Forest S, Sab K (1998) Cosserat overall modelling of heterogeneous materials. *Mechanics Research Communications* 25(4):449-454

[22] de Borst R (1993) A generalisation of J2 –flow theory for polar continua. *Comput Method in Appl M* 103:347-362

[23] Sansour C, Skatulla S, Zbib H (2010) A formulation for the micromorphic continuum at finite inelastic strains. *Int J Solids Struct* 47:1546–1554

[24] Isbuga V, Regueiro RA (2011) Three-dimensional finite element analysis of finite deformation micromorphic linear isotropic elasticity. *Int J Eng Sci* 49:1326–1336

[25] Tsiatas GC (2009) A new Kirchhoff plate model based on a modified couple stress theory. *Int J Solids Struct* 46:2757–2764

[26] Park SK, Gao X-L (2006) Bernoulli–Euler beam model based on a modified couple stress theory. *J Micromech Microeng* 16:2355–2359

[27] Lam DCC, Yang F, Chong ACM, Wang J, Tong P (2003) Experiments and theory in strain gradient elasticity. *J Mech Phys Solids* 51:1477–1508

[28] Bauer S, Schäfer M, Grammenoudis P, Tsakmakis Ch (2010) Three-dimensional finite elements for large deformation micropolar elasticity. *Comput Method Appl M* 199:2643–2654

[29] Chen W, Si J (2013) A model of composite laminated beam based on the global–local theory and new modified couple-stress theory. *Compos Struct* 103:99–107

[30] Fleck NA, Shu JY (1995) Microbuckle initiation in fibre composites: a finite element study. *J Mech Phys Solids* 43(12):1887–1918

[31] Lasota T, Burša J (2009) Size effect in computational simulations of experiments with composite materials. In *26th Symposium on Advances in Experimental Mechanics*. Montanuniversität Leoben, Austria 133-134. ISBN: 978-3-902544-02- 5

[32] Forest S, Sievert R (2006) Nonlinear microstrain theories. *Int J Solids Struct* 43:7224–7245

[33] Cosserat E, Cosserat F (1909) Théorie des corps déformables. A. Hermann et Fils, Paris

[34] Eringen AC (1962) Nonlinear Theory of Continuous Media. McGraw-Hill, New York

[35] Altenbach J, Altenbach H, Eremeyev VA (2010) On generalized Cosserat-type theories of plates and shells: a short review and bibliography. *Arch Appl Mech* 80:73–92

[36] Koiter WT (1964) Couple stresses in the theory of elasticity I and II. *Proc Kon Ned Akad Wetensch* 67:17–44

[37] Soldatos KP (2009) Azimuthal shear deformation of an ideal fibre-reinforced tube according to a second-gradient hyper-elasticity theory. In: Ambrosio J et al. (Eds.), *Proceedings of the Seventh EUROMECH Solid Mechanics Conference, Lisbon*

[38] Soldatos KP (2010) Second-gradient plane deformations of ideal fibre-reinforced materials: implications of hyper-elasticity theory. *J Eng Math* 68(1):99-127

[39] Soldatos KP (2012) On loss of ellipticity in second-gradient hyper-elasticity of fibre-reinforced materials. *Int J Nonlinear Mech* 47:117-127

[40] Pagano N J (1969) Exact solutions for composite laminates in cylindrical bending *J. Composite Materials* 3:398-411

[41] Spencer AJM (1984) Constitutive theory for strongly anisotropic solids. In: Spencer AJM (Ed.) *Continuum Theory of the Mechanics of Fibre-Reinforced Composites, CISM Courses and Lectures.* International Centre for Mechanical Sciences, Springer-Verlag, Wien

List of author's publications

Conference papers (in Scopus database)

[1] FEDOROVA, S.; BURŠA, J. Application of polar elasticity to the problem of pure bending of a thick plate. In *ECCOMAS Congress 2016 - Proceedings of the 7th European Congress on Computational Methods in Applied Sciences and Engineering.* Crete, Greece: National Technical University of Athens, 2016. p. 2162-2171. ISBN: 9786188284401.

[2] LASOTA, T.; BURŠA, J.; FEDOROVA, S. Constitutive equations and finite element formulation for anisotropic hyperelastic composites based on constrained Cosserat continuum. In *ECCOMAS 2012 - European Congress on Computational Methods in Applied Sciences and Engineering, e-Book Full Papers.* Vienna: Elsevier, 2012. p. 3379-3389. ISBN: 978-3-9502481-9-7.

[3] FEDOROVA, S.; LASOTA, T.; BURŠA, J.; SKÁCEL, P. Experimental verification of a constitutive model of fibre composite with hyperelastic matrix. In *EAN Proceedings 50th annual conference on experimental stress analysis.* Tábor: CTU Prague, 2012. p. 65-72. ISBN: 978-80-01-05060-6. (also in CPCI WoS)

Book chapter

FEDOROVA, S.; LASOTA, T.; BURŠA, J. Computational Modeling of Fiber Composites with Thick Fibers as Homogeneous Structures with Use of Couple Stress Theory. In *Design and Analysis of Reinforced Fiber Composites.* Pedro V. Marcal, Nobuki Yamagata (editors). Springer Cham, Heidelberg, New York, Dordrecht, London 2016. (24 pages). 2015. p. 25-47. ISBN: 978-3-319-20007-1, 3319200070, 9783319200071.

Conference abstracts

[1] FEDOROVA, S.; LASOTA, T.; BURŠA, J. *Application of couple-stress theory for description of large strain bending of fibre composites.* ICCS18 - 18th International Conference on Composite Structures, Lisbon - Portugal, June 15-18, 2015.

[2] LASOTA, T.; FEDOROVA, S.; BURŠA, J. *Constitutive and computational modelling of the effect of fibre bending resistance in reinforced elastomers.* 11th World Congress on Computational Mechanics (WCCM XI), 5th European Conference on Computational Mechanics (ECCM V), 6th European Conference on Computational Fluid Dynamics (ECFD VI), Barcelona - Spain, July 20-25, 2014.

[3] FEDOROVA, S.; LASOTA, T.; BURŠA, J. *Computational modelling of steel fibre reinforced elastomers based on couple stress theory.* Euromech Colloquium 551: "Fibre-reinforced Materials: Theory and Applications", Nottingham - UK, Sept 2-5, 2013.

[4] FEDOROVA, S. *Computational modelling of fibre-reinforced hyperelastic solids with fibre bending stiffness.* MSMF7 - Materials Structure & Micromechanics of Fracture, Brno – Czechia, July 1-3, 2013. ISBN: 978-80-214-4739-4.

CURRICULUM VITAE

Svitlana Fedorova

Email address: svtlnfdrv2@gmail.com

Education

2015 – 2018	PhD student, Brno University of Technology, combined form of study
2011 – 2015	PhD student, Brno University of Technology, presence form of study
2010	Diploma of Magister of Mechanics with honors major "Dynamics and Strength", National Technical University "Kharkiv Polytechnic Institute"

Academic internships

16.10.2015 - 23.11.2015	University of Nottingham, School of Mathematical Sciences
12.10.2014 - 15.11.2014	University of Nottingham, School of Mathematical Sciences
19.06.2014 - 17.07.2014	University of Nottingham, School of Mathematical Sciences
01.04.2010 - 30.04.2010	RWTH Aachen University, Department of Continuum Mechanics

Work Experience

2016 - present	Daido Metal, Analysis engineer